

Trajectory Tracking for Unmanned Air Vehicles With Velocity and Heading Rate Constraints

Wei Ren, *Student Member, IEEE*, and Randal W. Beard, *Senior Member, IEEE*

Abstract—This paper considers the problem of constrained nonlinear trajectory tracking control for unmanned air vehicles (UAVs). We assume that the UAV is equipped with longitudinal and lateral autopilots which reduces the 12-state model to a six-state model with altitude, heading, and velocity command inputs. One of the novel features of our approach is that we explicitly account for heading rate and velocity input constraints. For a UAV, the velocity is constrained to lie between two positive constants, and therefore presents particular challenges for the control design. We propose a control Lyapunov function (CLF) approach. We first introduce a CLF for the input constrained case, and then construct the set of all constrained inputs that are feasible with respect to this CLF. The control input is then selected from this “feasible” set. The proposed approach is applied to a simulation scenario, where the UAV is assigned to transition through several targets in the presence of multiple dynamic threats.

Index Terms—Control Lyapunov functions, input constraints, trajectory tracking, unmanned air vehicles.

I. INTRODUCTION

CONTROLLER design for nonlinear systems subject to input constraints offers both practical significance and theoretical challenges. Two effective approaches for the design of nonlinear controllers are control Lyapunov functions (CLFs) [1], [2] and receding horizon control (RHC)/model predictive control (MPC), [3], [4]. Both approaches can be extended to find control laws for nonlinear systems subject to certain input constraints. In [5] and [6], constrained CLFs are applied to construct stabilizing universal formulas, respectively, for systems with control inputs bounded in a unit ball and systems with a scalar control input that is positive and/or bounded. Input constraints can also be incorporated into the MPC framework, which is known as constrained MPC [4]. The issues limiting the utility of the RHC approach are its computation requirements and stability concerns.

In this paper, we consider the problem of constrained nonlinear tracking control for small fixed-wing unmanned air vehicles (UAVs). The inherent properties of fixed-wing UAVs impose the input constraints of positive-minimum velocity due to the stall conditions of the aircraft, bounded maximum velocity due to thrust limitations, and saturated heading rate due

to roll angle and pitch-rate constraints. Unmanned air vehicles (UAVs) equipped with low-level altitude-hold, velocity-hold, and heading-hold autopilots can be modeled by kinematic equations of motion that are similar to those of nonholonomic mobile robots. However, existing approaches for mobile robots [7]–[10] are not directly applicable to this problem since negative velocities are allowed in these approaches. This paper deals with the issue of tracking control for UAV kinematic models with physically motivated heading rate and velocity constraints. We approach the problem using constrained CLFs.

The first step is to propose a time-varying, constrained CLF for the kinematic model of the UAV. Following [11], the CLF is used to define a state-dependent time-varying set of feasible control values from which different controllers can be instantiated. Selection from this feasible control set guarantees accurate tracking as well as satisfaction of the saturation constraints. As noted in [11], different control strategies can be derived by selection from the feasible control set according to some auxiliary performance index. This approach introduces a great deal of flexibility to the tracking control problem. In this paper we propose an aggressive, i.e., high-gain selection scheme.

The motivation for this selection scheme is computational simplicity. It is worthwhile to mention that the existing CLF-based universal formulas introduced in [5], [6] are not feasible in the UAV case due to its special input constraints, that is, controls are constrained to lie in a time-varying rectangle.

The salient features of our approach are as follows. First, under the proposed framework, we allow the reference velocity and angular velocity to be piecewise continuous while other approaches to tracking control [9], [10] constrain them to be uniformly continuous in order to apply Barbalat’s lemma. Second, using different selection schemes, our approach can be used to derive a variety of other trajectory tracking strategies. Finally, it is computationally simple and can be implemented with a low-cost low-power microcontroller. To illustrate the effectiveness of the controller, we apply our approach to a scenario where the UAV is assigned to transition through several opportunities in the presence of dynamic hazards. Instead of following simple paths composed of straight lines and circles [9], [10], the UAV tracks a trajectory generated dynamically from the trajectory generator described in [12], which responds to the current, possibly time-varying, opportunity/hazard scenario.

II. PROBLEM STATEMENT

As shown in Fig. 1, the overall system architecture considered in this paper consists of five layers [13]: waypoint path planner (WPP), dynamic trajectory smoother (DTS), trajectory tracker (TT), longitudinal and lateral autopilots, and the UAV.

Manuscript received May 16, 2003; revised November 6, 2003. Manuscript received in final form January 26, 2004. Recommended by Associate Editor J. M. Buffington. This work was supported in part by the Air Force Office of Scientific Research under Grants F49620-01-1-0091 and F49620-02-C-0094, and in part by the Defense Advanced Research Projects Agency under Grant NBCH1020013.

The authors are with the Electrical and Computer Engineering Department, Brigham Young University, Provo, UT 84601 USA (e-mail: beard@ee.byu.edu).
Digital Object Identifier 10.1109/TCST.2004.826956

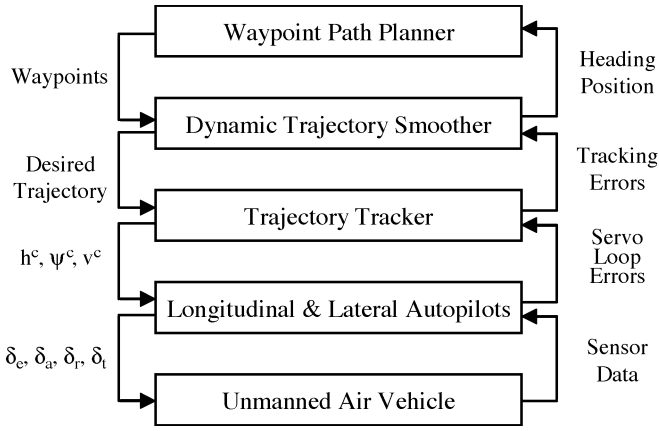


Fig. 1. System architecture.

The WPP generates waypoint paths (straight-line segments) that change in accordance with the dynamic environment consisting of the location of the UAV, the targets, and the dynamically changing threats. The DTS smoothes through these waypoints and produces a feasible time-parameterized reference trajectory where $(x_r(t), y_r(t))$ is the reference position, $\psi_r(t)$ is the reference heading, and $h_r(t)$ is the reference altitude. The TT outputs the velocity command v^c , heading command ψ^c , and altitude command h^c to the autopilots based on the desired trajectory. The autopilots then use these commands to control the elevator, δ_e , aileron, δ_a , rudder δ_r , and throttle δ_t , of the UAV [13]. In this paper, we focus on the Trajectory Tracker.

With the UAV equipped with standard autopilots, the resulting UAV/autopilot models are assumed to be first order for heading and Mach hold, and second order for altitude hold [14]. Letting (x, y) , ψ , v , and h denote the inertial position, heading angle, velocity, and altitude of the UAV, respectively, the kinematic equations of motion are given by

$$\begin{aligned}\dot{x} &= v \cos(\psi) \\ \dot{y} &= v \sin(\psi) \\ \dot{\psi} &= \alpha_\psi(\psi^c - \psi) \\ \dot{v} &= \alpha_v(v^c - v) \\ \ddot{h} &= -\alpha_h \dot{h} + \alpha_h(h^c - h)\end{aligned}\quad (1)$$

where ψ^c , v^c , and h^c are the commanded heading angle, velocity, and altitude to the autopilots, and α_* are positive constants associated with the autopilot [14].

Assuming that α_v is large relative to α_ψ , v converges to v^c quickly relative to the time-scale of the other dynamics. Therefore, the first four equations in (1) reduce to

$$\begin{aligned}\dot{x} &= v^c \cos(\psi) \\ \dot{y} &= v^c \sin(\psi) \\ \dot{\psi} &= \alpha_\psi(\psi^c - \psi).\end{aligned}\quad (2)$$

In the remainder of the paper, we assume that the altitude controller follows the design presented in [15], and focus on the design of the velocity and heading controller based on (2). Letting $\psi^c = \psi + (1/\alpha_\psi)\omega^c$, (2) becomes

$$\begin{aligned}\dot{x} &= v^c \cos(\psi) \\ \dot{y} &= v^c \sin(\psi) \\ \dot{\psi} &= \omega^c.\end{aligned}\quad (3)$$

The dynamics of the UAV impose the following input constraints

$$\mathcal{U}_1 = \{v^c, \omega^c | 0 < v_{\min} \leq v^c \leq v_{\max}, -\omega_{\max} \leq \omega^c \leq \omega_{\max}\}.\quad (4)$$

Note that if $v_{\min} = -v_{\max}$, then (3) is the same as the kinematic model for a mobile robot with similar input constraints.

We will assume that the desired reference trajectory $(x_r, y_r, \psi_r, v_r, \omega_r)$ produced by the DTS satisfies

$$\begin{aligned}\dot{x}_r &= v_r \cos(\psi_r) \\ \dot{y}_r &= v_r \sin(\psi_r) \\ \dot{\psi}_r &= \omega_r\end{aligned}$$

where v_r and ω_r are piecewise continuous and satisfy the constraints

$$\begin{aligned}v_{\min} + \epsilon_v &\leq v_r \leq v_{\max} - \epsilon_v \\ -\omega_{\max} + \epsilon_\omega &\leq \omega_r \leq \omega_{\max} - \epsilon_\omega\end{aligned}\quad (5)$$

where ϵ_v and ϵ_ω are positive control parameters. The inclusion of ϵ_* in the constraints of the reference trajectory generator, guarantees that there is sufficient control authority to track the trajectory. We will see that as ϵ_* approach zero, the feasible control set vanishes. The control objective is to find feasible control inputs v^c and ω^c such that $|x_r - x| + |y_r - y| + |\psi_r - \psi| \rightarrow 0$ as $t \rightarrow \infty$.

Transforming the tracking errors expressed in the inertial frame to the UAV frame, the error coordinates can be denoted as [16]

$$\begin{bmatrix} x_e \\ y_e \\ \psi_e \end{bmatrix} = \begin{bmatrix} \cos(\psi) & \sin(\psi) & 0 \\ -\sin(\psi) & \cos(\psi) & 0 \\ 0 & 0 & 1 \end{bmatrix} \begin{bmatrix} x_r - x \\ y_r - y \\ \psi_r - \psi \end{bmatrix}.\quad (6)$$

Accordingly, the tracking-error model can be represented as

$$\begin{aligned}\dot{x}_e &= \omega^c y_e - v^c + v_r \cos(\psi_e) \\ \dot{y}_e &= -\omega^c x_e + v_r \sin(\psi_e) \\ \dot{\psi}_e &= \omega_r - \omega^c.\end{aligned}\quad (7)$$

Following [10], (7) can be simplified as

$$\begin{aligned}\dot{x}_0 &= u_0 \\ \dot{x}_1 &= (\omega_r - u_0)x_2 + v_r \sin(x_0) \\ \dot{x}_2 &= -(\omega_r - u_0)x_1 + u_1\end{aligned}\quad (8)$$

where

$$(x_0, x_1, x_2) \triangleq (\psi_e, y_e, -x_e)\quad (9)$$

and $u_0 \triangleq \omega_r - \omega^c$ and $u_1 \triangleq v^c - v_r \cos(x_0)$.

The input constraints under the transformation become

$$\mathcal{U}_2 = \{u_0, u_1 | \underline{\omega} \leq u_0 \leq \bar{\omega}, \underline{v} \leq u_1 \leq \bar{v}\}\quad (10)$$

where $\underline{\omega} \triangleq \omega_r - \omega_{\max}$, $\bar{\omega} \triangleq \omega_r + \omega_{\max}$, $\underline{v} \triangleq v_{\min} - v_r \cos(x_0)$, and $\bar{v} \triangleq v_{\max} - v_r \cos(x_0)$ are time-varying.

Obviously, (6) and (9) are invertible transformations, which means that $(x_0, x_1, x_2) = (0, 0, 0)$ is equivalent to $(x_e, y_e, \psi_e) = (0, 0, 0)$, or in other words $(x_r, y_r, \psi_r) = (x, y, \psi)$. Therefore, the original tracking control objective is converted to a stabilization objective. That is, our goal is to find feasible control inputs u_0 and u_1 to stabilize x_0 , x_1 , and x_2 .

Note from (8) that when both x_0 and x_2 go to zero, x_1 becomes uncontrollable. To avoid this situation we introduce another change of variables. Let $\bar{x}_0 = mx_0 + x_1/\pi_1$, where $m > 0$ and $\pi_1 \triangleq \sqrt{x_1^2 + x_2^2 + 1}$. Accordingly, $x_0 = \bar{x}_0/m - x_1/m\pi_1$. Obviously, $(\bar{x}_0, x_1, x_2) = (0, 0, 0)$ is equivalent to $(x_0, x_1, x_2) = (0, 0, 0)$. Therefore, it is sufficient to find control inputs u_0 and u_1 to stabilize \bar{x}_0 , x_1 , and x_2 . With the same input constraints (10), (8) can be rewritten as

$$\dot{x} = f_1(t, x) + g_1(t, x)[u_0, u_1]^T \quad (11)$$

where $x = [\bar{x}_0, x_1, x_2]^T$

$$f_1(t, x) = \begin{bmatrix} \frac{x_2}{\pi_1}\omega_r + \frac{1+x_2^2}{\pi_1^3}v_r \sin\left(\frac{\bar{x}_0}{m} - \frac{x_1}{m\pi_1}\right) \\ x_2\omega_r + v_r \sin\left(\frac{\bar{x}_0}{m} - \frac{x_1}{m\pi_1}\right) \\ -\omega_r x_1 \end{bmatrix}$$

and

$$g_1(t, x) = \begin{bmatrix} m - \frac{x_2}{\pi_1} & -\frac{x_1 x_2}{\pi_1^3} \\ -x_2 & 0 \\ x_1 & 1 \end{bmatrix}.$$

III. CLF FOR TRACKING CONTROL WITH SATURATION CONSTRAINTS

In this section, we find a valid CLF for UAV trajectory tracking with input constraints. Consider the following class of affine nonlinear time-varying systems

$$\dot{x} = f(t, x) + g(t, x)u \quad (12)$$

where $x \in \mathbb{R}^n$, $u \in \mathbb{R}^m$, and $f : \mathbb{R}_+ \times \mathbb{R}^n \rightarrow \mathbb{R}^n$ and $g : \mathbb{R}_+ \times \mathbb{R}^n \rightarrow \mathbb{R}^{n \times m}$ are locally Lipschitz in x and piecewise continuous in t .

Definition 1: (See [1]) A continuously differentiable function $V : \mathbb{R}_+ \times \mathbb{R}^n \rightarrow \mathbb{R}$ is a control Lyapunov function (CLF) for system (12) with input constraints $u \in \mathcal{U} \subset \mathbb{R}^m$ if it is positive-definite, decrescent, radially unbounded in x , and satisfies

$$\inf_{u \in \mathcal{U}} \left\{ \frac{\partial V}{\partial t} + \frac{\partial V}{\partial x} (f(t, x) + g(t, x)u) \right\} \leq -W(x) \quad (13)$$

$\forall x \neq 0$ and $\forall t \geq 0$ where $W(x)$ is a continuous positive-definite function.

In order to find a CLF with bounded input constraints, we prefer the partial derivative of V to be bounded. Accordingly, we have the following lemma.

Lemma 2: If $P(x) = \sqrt{x^T x + 1} - 1$, then $P(x)$ is continuously differentiable, radially unbounded, positive-definite, and $\|\partial P/\partial x\| \leq 1$.

Proof: Trivial. \blacksquare

Lemma 2 will be used to construct a CLF for system (11). The following lemma defines a continuous positive-definite function that will be used in the construction of the CLF.

Lemma 3: Let

$$W(x) = \gamma_0 \left(\frac{\bar{x}_0}{\pi_2} \right)^2 + \gamma_1 k_1 (v_{\min} + \epsilon_v) \frac{x_1}{\pi_1} \sin\left(\frac{x_1}{m\pi_1}\right) + \gamma_2 \left(k_1 - \frac{1}{2} \right) \left(\frac{x_2}{\pi_1} \right)^2 \left((v_{\min} + \epsilon_v) \cos\left(\frac{x_1}{m\pi_1}\right) - v_{\min} \right) \quad (14)$$

where $\pi_2 \triangleq \sqrt{\bar{x}_0^2 + 1}$. If $k_1 > 1/2$, $\gamma_i > 0$, and $m > 2/\cos^{-1}(v_{\min}/(v_{\min} + \epsilon_v))$, then $W(x)$ is continuous and positive-definite.

Proof: Since W is a composition of continuous functions, it is continuous. The first term in (14) is clearly positive and zero if and only if $\bar{x}_0 = 0$. The second term in (14) is nonnegative if $|x_1/m\pi_1| < \pi$. But since

$$\left| \frac{x_1}{m\pi_1} \right| < \frac{1}{m} < \frac{\cos^{-1}\left(\frac{v_{\min}}{v_{\min} + \epsilon_v}\right)}{2} < \frac{\pi}{4} \quad (15)$$

the second term is positive and zero if and only if $x_1 = 0$. Since

$$\begin{aligned} \left| \frac{x_1}{m\pi_1} \right| &< \frac{\cos^{-1}\left(\frac{v_{\min}}{v_{\min} + \epsilon_v}\right)}{2} < \cos^{-1}\left(\frac{v_{\min}}{v_{\min} + \epsilon_v}\right) \\ \implies \cos\left(\frac{x_1}{m\pi_1}\right) &> \frac{v_{\min}}{v_{\min} + \epsilon_v} \\ \iff (v_{\min} + \epsilon_v) \cos\left(\frac{x_1}{m\pi_1}\right) - v_{\min} &> 0 \end{aligned} \quad (16)$$

the third term in (14) is positive and zero if and only if $x_2 = 0$. \blacksquare

The following theorem defines a valid CLF for UAV trajectory tracking with input constraints.

Theorem 4: The function

$$\begin{aligned} V &= P(\bar{x}_0) + k_1 P\begin{pmatrix} x_1 \\ x_2 \end{pmatrix} \\ &= \sqrt{\bar{x}_0^2 + 1} + k_1 \sqrt{x_1^2 + x_2^2 + 1} - (1 + k_1) \end{aligned}$$

satisfies $\inf_{u \in \mathcal{U}} \{(\partial V/\partial x)(f_1 + g_1 u)\} \leq -W(x)$ (that is, V is a CLF for system (11) with input constraints (10)), if $W(x)$ is given by Lemma 3, $0 < \gamma_1 < 1$, $0 < \gamma_2 < 1$ and

$$m > \max \left\{ M_0, 1 + \frac{d_2}{\epsilon_v} \right\}$$

where

$$M_0 \triangleq \max \left\{ \frac{2}{\cos^{-1}\left(\frac{v_{\min}}{v_{\min} + \epsilon_v}\right)}, 1 + \sqrt{2} \frac{d_1}{\epsilon_v} \right\} \quad (17)$$

$$\begin{aligned} d_1 &\triangleq \left(k_1 + \frac{1}{2} \right) [2v_{\max} - \epsilon_v] + \gamma_2 \left(k_1 - \frac{1}{2} \right) \epsilon_v \\ &\quad + k_1 [(v_{\max} - \epsilon_v) + \gamma_1 (v_{\min} + \epsilon_v)] \\ &\quad + (\omega_{\max} - \epsilon_v) + (v_{\max} - \epsilon_v) + \gamma_0 \end{aligned} \quad (18)$$

$$\begin{aligned} d_2 &\triangleq (v_{\max} - \epsilon_v) \left[\sqrt{2} \left(k_1 - \frac{1}{2} \right) \frac{M_2}{M_0} + \sqrt{2} k_1 \frac{M_1}{M_0} + 1 \right] \\ &\quad + (\omega_{\max} - \epsilon_v) + \gamma_0 \end{aligned} \quad (19)$$

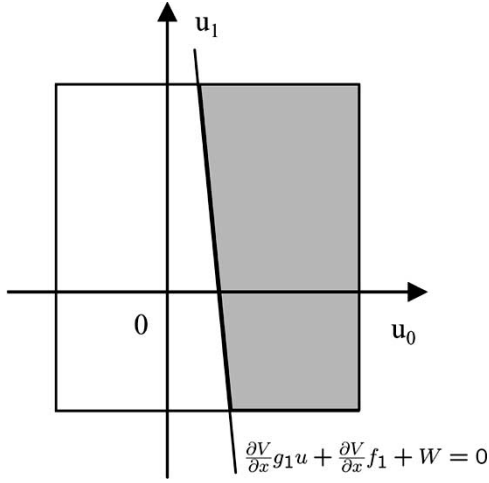


Fig. 2. The feasible control set $\mathcal{F}(t, x)$ at some time $t = \hat{t}$.

and

$$M_1 \triangleq \sup_{\substack{0 < |\alpha| < \frac{1}{M_0} \\ |\beta| < \frac{1}{M_0}}} \left| \frac{\sin(\alpha - \beta) + \sin(\beta)}{\alpha} \right| \quad (20)$$

$$M_2 \triangleq \sup_{\substack{0 < |\alpha| < \frac{1}{M_0} \\ |\beta| < \frac{1}{M_0}}} \left| \frac{\cos(\beta) - \cos(\alpha - \beta)}{\alpha} \right|. \quad (21)$$

Proof: See Appendix I. ■

It is straightforward to show that M_1 and M_2 in (20) and (21) are bounded as $|\alpha|$ approaches both 0 and $1/M_0$. Therefore, M_1 and M_2 are finite and can be found by standard numerical methods.

Theorem 4 demonstrates that V is a valid CLF for system (11) under saturation constraints (10). Note from the proof in Appendix I that a very conservative upper bound is found for m , which can be much smaller in practice.

IV. NONLINEAR TRACKING CONTROL BASED ON CLF

With the CLF given in Theorem 4, our goal in this section is to find a family of feasible tracking control laws based on this CLF.

Define the feasible control set as

$$\mathcal{F}(t, x) = \left\{ u \in \mathcal{U}_2 \left| \frac{\partial V}{\partial x} g_1(t, x)u + \frac{\partial V}{\partial x} f_1(t, x) \leq -W(x) \right. \right\}$$

where V is given in Theorem 4 and $W(x)$ is given in Lemma 3. Note that the fact that V is a constrained CLF for system (11) guarantees that $\mathcal{F}(t, x)$ is nonempty for any t and x .

Fig. 2 shows the feasible control set at some time $t = \hat{t}$. The line denoted by $(\partial V/\partial x)g_1u + (\partial V/\partial x)f_1 + W = 0$ separates the 2-D control space into two halves, where the half plane $(\partial V/\partial x)g_1u + (\partial V/\partial x)f_1 + W \leq 0$ (the entire right plane in Fig. 2) represents the unconstrained stabilizing control set. The input constraints (10) produce a time-varying rectangle in the $u_0 - u_1$ plane. The shaded area represents the stabilizing controls which also satisfy input constraints (10), that is, the feasible control set $\mathcal{F}(t, x)$.

We have the following theorem.

Theorem 5: If the time-varying feedback control law $k(t, x)$ satisfies

- 1) $k(t, 0) = 0$,
- 2) $k(t, x) \in \mathcal{F}(t, x)$, $\forall x \neq 0$,
- 3) $k(t, x)$ is locally Lipschitz in x and piecewise continuous in t , $\forall x \neq 0$ and $\forall t \geq 0$,

then this control solves the tracking problem with input constraints, that is, $|x_r - x| + |y_r - y| + |\psi_r - \psi| \rightarrow 0$ as $t \rightarrow \infty$.

Proof: See [11]. ■

There are an infinite number of possibilities for selecting a feedback strategy that satisfies Theorem 5. In this paper we will investigate the performance of an aggressive selection scheme that chooses the maximum allowable u_0 and u_1 outside of a region close to the origin. This scheme can be interpreted as a high-gain scheme with saturation. Define the saturation function as

$$\text{sat}(a, b, c) = \begin{cases} b & a < b \\ a & b \leq a \leq c \\ c & a > c \end{cases}$$

where it is assumed that $b < c$.

Lemma 6: If

$$u_0 = \text{sat}(-\eta_\omega \bar{x}_0, \underline{\omega}, \bar{\omega}) \quad (22)$$

$$u_1 = \text{sat}(-\eta_v x_2, \underline{v}, \bar{v}) \quad (23)$$

where $\eta_\omega > \kappa_\omega$ and $\eta_v > \kappa_v$ and κ_ω and κ_v are defined in Appendix II, then $k_{\text{sat}}(t, x) = [u_0, u_1]^T$ satisfies the conditions of Theorem 5.

Proof: See Appendix II. ■

In Lemma 6, we used a simple control law that stays in the feasible control set. Other continuous saturation functions like atan , tanh are also possible as long as they stay in the feasible control set. In the case of v_r and ω_r being uniformly continuous, it is also possible to use geometrical strategies to find feasible control laws (e.g., choose the geometrical center of the feasible control set $\mathcal{F}(t, x)$ as feasible controls).

Note that the commanded velocity and heading rate to the autopilots are defined as $v^c \triangleq u_1 + v_r \cos(x_0)$ and $\omega^c \triangleq \omega_r - u_0$.

Physically, there may exist perturbation terms in system (11) due to uncertainties and external disturbances. We address the issue of uncertainties and disturbances under the input-to-state (ISS) framework [17].

Consider the system

$$\dot{x} = f(t, x) + g(t, x)u + d \quad (24)$$

which introduces a perturbation term $d \in \mathbb{R}^n$ to the nominal system (12).

Definition 7: [18] A continuously differentiable function $V : \mathbb{R}_+ \times \mathbb{R}^n \rightarrow \mathbb{R}$ is an ISS-CLF for system (24) if it is positive-definite, decrescent, radially unbounded in x and there exist class \mathcal{K} functions $\chi(\cdot)$ and $\rho(\cdot)$ such that

$$\inf_{u \in \mathbb{R}^m} \frac{\partial V}{\partial t} + \frac{\partial V}{\partial x} f + \frac{\partial V}{\partial x} g u + \frac{\partial V}{\partial x} d \leq -\chi(\|x\|) \quad \forall \|x\| \geq \rho(\|d\|).$$

Given $W(x)$ in (14), there exists a class \mathcal{K} function χ_w such that $\chi_w(\|x\|) \leq W(x)$, $\forall x$ ([19], Lemma 3.5).

Lemma 8: Let $\mu = \sup_{\|x\| \rightarrow \infty} \chi_w(\|x\|)$ and $b_1 = [1, k_1, k_1]^T$. If $\|d\| < \lambda\mu/\|b_1\|$, where $0 < \lambda < 1$, then $V(x)$ is also an ISS-CLF with input constraints (10) for system

$$\dot{x} = f_1(t, x) + g_1(t, x)u + d \quad (25)$$

where d is the perturbation term to the nominal system (11).

Proof: Note that $\frac{\partial V}{\partial x} = [\bar{x}_0/\pi_2, k_1(x_1/\pi_1), k_1(x_2/\pi_1)]$, where $|\bar{x}_0/\pi_2| < 1$, $|x_1/\pi_1| < 1$, and $|x_2/\pi_1| < 1$.

It can be seen that

$$\begin{aligned} & \inf_{u \in \mathcal{U}_2} \frac{\partial V}{\partial x} f_1 + \frac{\partial V}{\partial x} g_1 u + \frac{\partial V}{\partial x} d \\ & \leq -W(x) + \left\| \frac{\partial V}{\partial x} d \right\| \\ & \leq -(1-\lambda)\chi_w(\|x\|) - \lambda\alpha_w(\|x\|) + \|b_1\| \|d\| \\ & \leq -(1-\lambda)\chi_w(\|x\|), \quad \forall \|x\| \geq \alpha_w^{-1} \left(\frac{\|b_1\| \|d\|}{\lambda} \right). \end{aligned}$$

Note that $\alpha_w^{-1}(\cdot)$ in the last inequality is also a class \mathcal{K} function of $\|d\|$ and is well defined since $\|b_1\| \|d\| / \lambda \leq \mu$. ■

Note that here $\chi_w(\cdot)$ is a class \mathcal{K} function instead of a class \mathcal{K}_∞ function, which in turn imposes constraints for $\|d\|$. This can be explained from the constrained input perspective. In the case of $d = 0$, the derivative of the CLF cannot approach $-\infty$ as the tracking errors approach ∞ even with maximum control authority due to the saturated controls. As a result, $\chi_w(\cdot)$ can only be a class \mathcal{K} function given the input constraints. Also note that with control inputs given by (22) and (23) $V(x)$ is an ISS-Lyapunov function under the assumptions of Lemma 8.

It is obvious that the commanded control v^c and ω^c rely on the state measurement x , y , and ψ . Due to measurement noise, there exist input uncertainties for $[v^c, \omega^c]^T$. Equivalently, we may consider input uncertainties for $[u_0, u_1]^T$ in system (11). We denote the actual control input to system (11) as $u = [u_0 + \Delta u_0, u_1 + \Delta u_1]^T$, where Δu_0 and Δu_1 represent the uncertainties. Due to saturation constraints, we know that $|\Delta u_0| \leq 2\omega_{\max}$ and $|\Delta u_1| \leq v_{\max} - v_{\min}$.

We have the following lemma considering input uncertainties.

Lemma 9: Let $b_2 = [m + 1, k_1 + 1/2]^T$ and $\Delta u = [\Delta u_0, \Delta u_1]^T$. If $\|\Delta u\| < \lambda\mu/\|b_2\|$, where $0 < \lambda < 1$, then $V(x)$ is an ISS-Lyapunov function for system (11) with control inputs given by (22) and (23) and $d = g_1 \Delta u$.

Proof: Noting that

$$\frac{\partial V}{\partial x} g_1 = \left[\left(m - \frac{x_2}{\pi_1} \right) \frac{\bar{x}_0}{\pi_2}, -\frac{\bar{x}_0}{\pi_2} \frac{x_1 x_2}{\pi_1^3} + k_1 \frac{x_2}{\pi_1} \right]$$

where $|(m - x_2/\pi_1)(\bar{x}_0/\pi_2)| < m + 1$, and $|-(\bar{x}_0/\pi_2)(x_1 x_2/\pi_1^3) + k_1(x_2/\pi_1)| < k_1 + 1/2$, the result then directly follows Lemma 8. ■

One advantage of the CLF-based approach used in this paper is that it only requires v_r and ω_r to be piecewise continuous instead of being uniformly continuous, which results in wider

TABLE I
PARAMETER VALUES USED IN SIMULATION

Parameter	Value	Parameter	Value
v_{\min}	8.0 (m/s)	v_{\max}	13.0 (m/s)
ω_{\max}	0.671 (rad/s)	ϵ_v	1.5 (m/s)
ϵ_ω	0.2 (rad/s)	v_r	$\in [9.5, 11.5]$ (m/s)
ω_r	$\in [-0.471, 0.471]$ (rad/s)	α_ψ	0.55
α_v	0.192	m	1
k_1	2	$\gamma_0, \gamma_1, \gamma_2$	0.5
η_0	10	η_1	10

potential applications than other approaches which require uniform continuity. The other advantage is that it provides the possibility to use other advanced strategies to choose feasible controls from $\mathcal{F}(t, x)$. For example, at each time t , a feasible control may be generated from $\mathcal{F}(t, x)$ while optimizing some performance index function or minimizing some cost function at the same time. This may introduce more flexibility and benefits to the tracking control problem than specifying a fixed control law in advance. In addition, it is also possible to propose a sub-optimal controller from $\mathcal{F}(t, x)$ based on the combination of model predictive techniques and the tracking CLF.

Although the approach in this paper is designed specifically for system (3), the design strategy can be applied more generally. If a constrained control Lyapunov function (CLF) can be found for a system with polytopic input constraints, the feasible control set that defines all the stabilizing controls with respect to the CLF satisfying the input constraints can be specified accordingly. Ref. [11] provides a complete parametrization of the unconstrained stabilizing controls with respect to a certain CLF. Following this idea, a direct parametrization of the feasible control set or selection from the feasible control set is applicable, e.g., finding the geometric mean of the feasible control set or a parametrization based on the vertices of the feasible control set (a polygon in this case).

V. SIMULATION RESULTS

In this section, we simulate a scenario where a UAV is assigned to transition through several known targets in the presence of dynamic threats. The parameters used in the simulation are given in Table I, which are the parameters for a three foot wingspan UAV used at Brigham Young University, Provo, UT. The simulation results in this section are based on a full six-DOF twelve-state model. Note that the value for m is much lower than the theoretical lower bound defined in Theorem 4. However, as we will see in the following, the saturation controller works well using this value, which implies the robustness of the controller to parameter variations.

Fig. 3 shows the reference trajectory generated by the dynamic trajectory smoother described in [12] and the actual trajectories generated by the saturation controller proposed in Lemma 6, and a controller based on the state-dependent Riccati equation (SDRE) approach [20], respectively. We note that the SDRE controller has been saturated to satisfy the input constraints. The dots denote threat locations to be avoided. Each trajectory at $t = 0$ is denoted by a circle while each trajectory at $t = 30$ is denoted by a square. Also each trajectory at $t = \{6, 12, 18, 24\}$ is denoted by a plus symbol. The trajectory tracking errors are plotted in Fig. 4. Note that

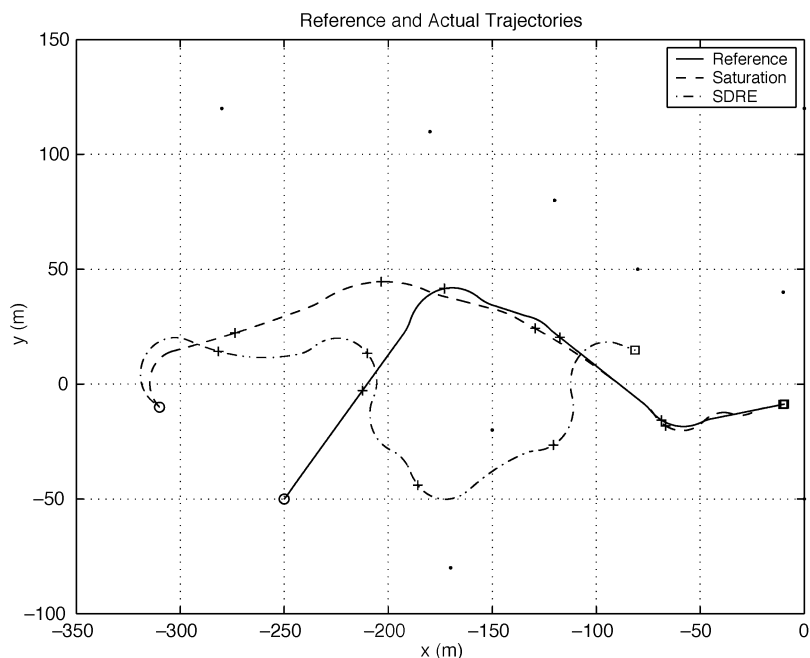


Fig. 3. The reference and actual trajectories of the six-DOF model.

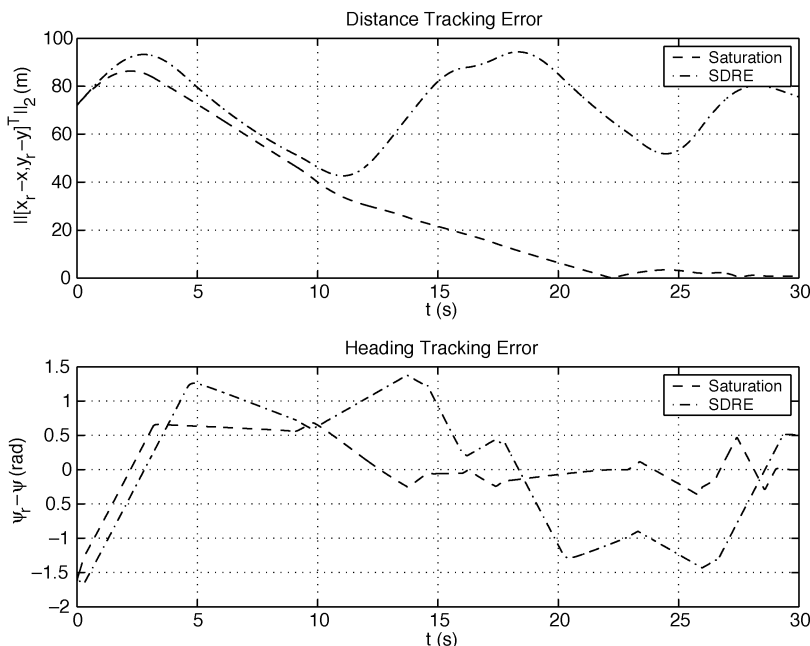


Fig. 4. The trajectory tracking errors of the six-DOF model.

the performance of the SDRE controller is much worse than that of the saturation controller since the SDRE design does not account for input constraints explicitly. In fact, the SDRE controller is not guaranteed to stay in the feasible control set. Without input constraints, the SDRE controller can achieve much better performance at the expense of huge velocity and heading rate commands. Fig. 5 shows the reference control inputs v_r and ω_r and commanded control inputs v^c and ω^c . Obviously, ω_r is only piecewise continuous instead of being uniformly continuous. The reference control inputs generated by the trajectory generator satisfy their constraints, respectively.

We can also see that v^c and ω^c satisfy their input constraints, respectively.

Fig. 6 shows the reference trajectory and the actual trajectory of the six-DOF model using the saturation controller under model uncertainties and disturbances. As in Fig. 3, a circle denotes the starting point of a trajectory and a square denotes the ending point. A diamond symbol denotes the trajectory at $t = \{10, 20, 30, 40\}$. Fig. 7 shows the corresponding tracking errors. Here each sensor measurement is corrupted with zero mean white noise. We can see that the saturation controller is robust to model uncertainties and disturbances.

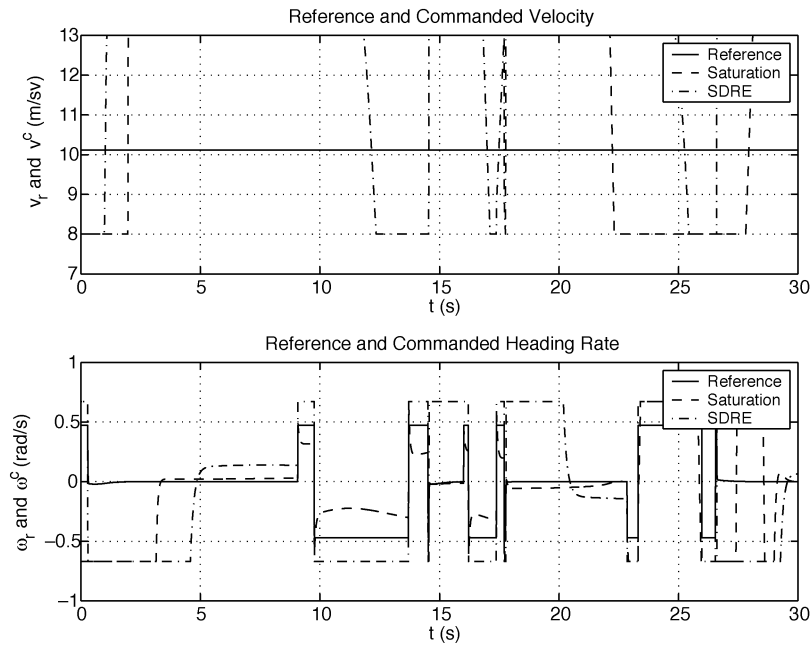


Fig. 5. The reference and commanded control inputs of the six-DOF model.

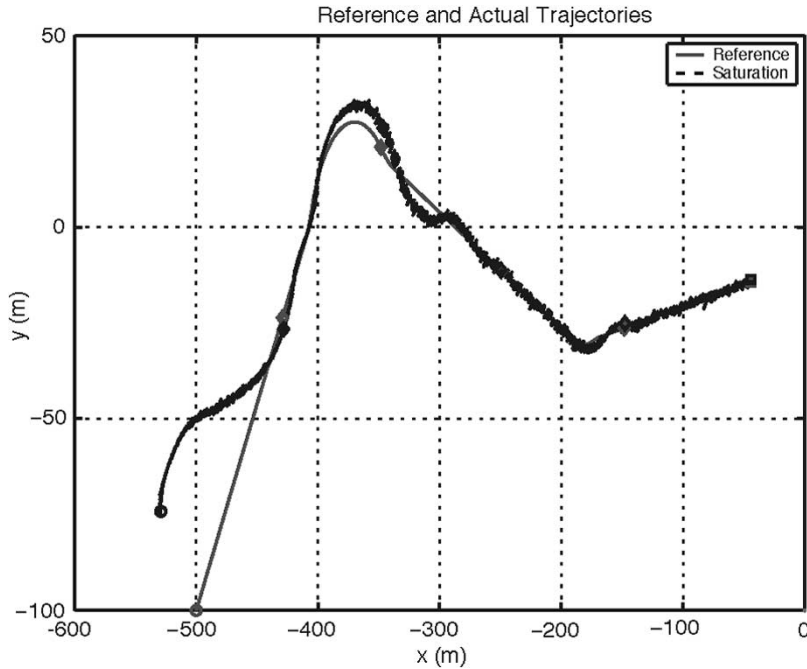


Fig. 6. The simulation scenario of the six-DOF model with model uncertainties and disturbances.

VI. CONCLUSION

A tracking CLF for a UAV kinematic model with input constraints is derived. Based on this CLF, a feasible control set is formed. This feasible control set facilitates the generation of a variety of feasible control strategies that not only guarantee accurate tracking but also optimize auxiliary performance functions. A simple saturation control strategy generated from the feasible control set was used and applied to a nontrivial simulation scenario.

APPENDIX I PROOF OF THEOREM 4

Obviously V is positive-definite, decreascent, and radially unbounded, therefore, it remains to show that $\dot{V} + W_3 \leq 0$ for all x .

Differentiating V and setting $u_0 = -\epsilon_\omega \text{sign}(\bar{x}_0)$, we obtain the following expression after some algebraic manipulation:

$$\dot{V} + W_3(x) = -\epsilon_\omega \frac{|\bar{x}_0|}{\pi_2} \left(m - \frac{x_2}{\pi_1} \right) + \sigma_1 u_1 + \sigma_2 + \sigma_3 + \sigma_4 \quad (26)$$

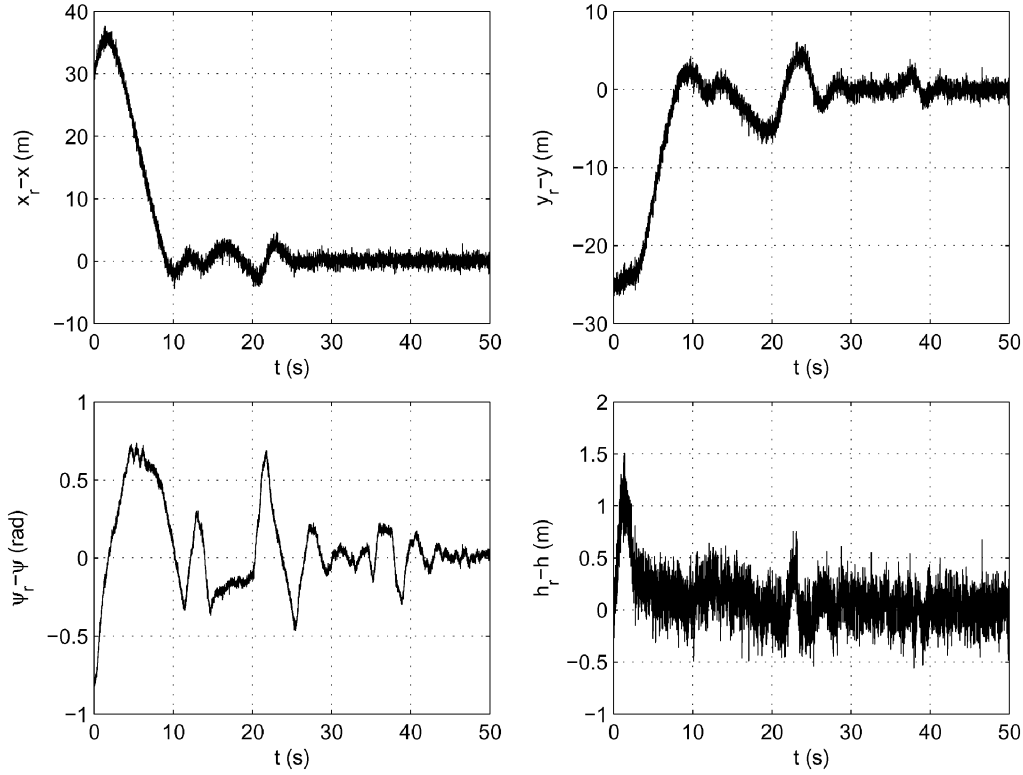


Fig. 7. The trajectory tracking errors of the six-DOF model with model uncertainties and disturbances.

where

$$\begin{aligned}\sigma_1 &= \left(k_1 - \frac{\bar{x}_0 x_1}{\pi_2 \pi_1^2}\right) \left(\frac{x_2}{\pi_1}\right) \\ \sigma_2 &= \gamma_2 \left(k_1 - \frac{1}{2}\right) \left(\frac{x_2}{\pi_1}\right)^2 \left[(v_{\min} + \epsilon_v) \cos\left(\frac{x_1}{m\pi_1}\right) - v_{\min} \right] \\ \sigma_3 &= k_1 \left(\frac{x_1}{\pi_1}\right) \left[v_r \sin\left(\frac{\bar{x}_0}{m} - \frac{x_1}{m\pi_1}\right) + \gamma_1 (v_{\min} + \epsilon_v) \sin\left(\frac{x_1}{m\pi_1}\right) \right] \\ \sigma_4 &= \left(\frac{\bar{x}_0}{\pi_2}\right) \left[\frac{x_2}{\pi_1} \omega_r + \frac{1+x_2^2}{\pi_1^3} v_r \sin\left(\frac{\bar{x}_0}{m} - \frac{x_1}{m\pi_1}\right) + \gamma_0 \left(\frac{\bar{x}_0}{\pi_2}\right) \right].\end{aligned}$$

Three cases will be considered with respect to \bar{x}_0 .

Case 1) $|\bar{x}_0| \geq 1$. Since $|\bar{x}_0/\pi_2| < 1$, $|x_1/\pi_1^2| < 1/2$, and $|x_2/\pi_1| < 1$, we know that $|\sigma_1| \leq (k_1 + 1/2)$. Note that

$$\begin{aligned}\sigma_1 u_1 &\leq \left(k_1 + \frac{1}{2}\right) (2v_{\max} - \epsilon_v) \\ \sigma_2 &\leq \gamma_2 \left(k_1 - \frac{1}{2}\right) \epsilon_v \\ \sigma_3 &\leq k_1 [(v_{\max} - \epsilon_v) + \gamma_1 (v_{\min} + \epsilon_v)] \\ \sigma_4 &\leq (\omega_{\max} - \epsilon_\omega) + (v_{\max} - \epsilon_v) + \gamma_0.\end{aligned}$$

Since $m > 1 + \sqrt{2}d_1/\epsilon_\omega$, we get that

$$\begin{aligned}\dot{V} + W_3 &\leq -\epsilon_\omega \frac{|\bar{x}_0|}{\pi_2} (m-1) + d_1 \\ &\leq -\frac{\epsilon_\omega}{\sqrt{2}} (m-1) + d_1 < 0\end{aligned}$$

where the second inequality comes from $|\bar{x}_0|/\pi_2 \geq 1/\sqrt{2}$ since $|\bar{x}_0| \geq 1$.

Case 2) $0 < |\bar{x}_0| < 1$. Eq. (26) can be arranged as

$$\dot{V} + W_3 = \frac{|\bar{x}_0|}{\pi_2} \left\{ -\epsilon_\omega \left(m - \frac{x_2}{\pi_1}\right) + \frac{\pi_2}{|\bar{x}_0|} [\sigma_1 u_1 + \sigma_2 + \sigma_3 + \sigma_4] \right\}.$$

We will show that

$$d_2 \geq \frac{\pi_2}{|\bar{x}_0|} (\sigma_1 u_1 + \sigma_2) + \frac{\pi_2}{|\bar{x}_0|} \sigma_3 + \frac{\pi_2}{|\bar{x}_0|} \sigma_4 \quad (27)$$

which implies that $m > 1 + d_2/\epsilon_\omega$ guarantees that $\dot{V} + W_3 \leq 0$.

Set

$$u_1 = \begin{cases} v_{\min} - v_r \cos\left(\frac{\bar{x}_0}{m} - \frac{x_1}{m\pi_1}\right) & x_2 \geq 0 \\ v_{\max} - v_r \cos\left(\frac{\bar{x}_0}{m} - \frac{x_1}{m\pi_1}\right) & x_2 < 0. \end{cases} \quad (28)$$

For the first term in (27), consider the following two cases with regard to x_2 .

1) $x_2 \geq 0$. Noting that $(x_2/\pi_1)^2 \leq |x_2|/\pi_1$ and

$$\begin{aligned}\left| \frac{\bar{x}_0}{m} - \frac{x_1}{m\pi_1} \right| &< \frac{2}{m} < \cos^{-1}\left(\frac{v_{\min}}{v_{\min} + \epsilon_v}\right) \\ \Rightarrow v_{\min} - v_r \cos\left(\frac{\bar{x}_0}{m} - \frac{x_1}{m\pi_1}\right) &< 0\end{aligned} \quad (29)$$

$$\begin{aligned}\left| \frac{\bar{x}_0 x_1}{\pi_2 \pi_1^2} \right| &< \frac{1}{2} \\ \Rightarrow \left(k_1 - \frac{\bar{x}_0 x_1}{\pi_2 \pi_1^2}\right) &> \left(k - \frac{1}{2}\right)\end{aligned} \quad (30)$$

$$\begin{aligned}\cos\left(\frac{x_1}{m\pi_1}\right) &> 0 \\ \Rightarrow (v_{\min} + \epsilon_v) \cos\left(\frac{x_1}{m\pi_1}\right) - v_{\min} \\ &\leq v_r \cos\left(\frac{x_1}{m\pi_1}\right) - v_{\min},\end{aligned} \quad (31)$$

the first term in (27) can be bounded as follows:

$$\begin{aligned}
& \frac{\pi_2}{|\bar{x}_0|} (\sigma_1 u_1 + \sigma_2) \\
&= \frac{\pi_2}{|\bar{x}_0|} \left\{ \left(k_1 - \frac{\bar{x}_0 x_1}{\pi_2 \pi_1^2} \right) \left(\frac{|x_2|}{\pi_1} \right) \right. \\
&\quad \times \left[v_{\min} - v_r \cos \left(\frac{\bar{x}_0}{m} - \frac{x_1}{m\pi_1} \right) \right] + \gamma_2 \left(k_1 - \frac{1}{2} \right) \\
&\quad \times \left. \left(\frac{x_2}{\pi_1} \right)^2 \left[(v_{\min} + \epsilon_v) \cos \left(\frac{x_1}{m\pi_1} \right) - v_{\min} \right] \right\} \\
&\leq \frac{\pi_2}{|\bar{x}_0|} \left\{ \left(k_1 - \frac{1}{2} \right) \left(\frac{|x_2|}{\pi_1} \right) \left[v_{\min} - v_r \cos \left(\frac{\bar{x}_0}{m} - \frac{x_1}{m\pi_1} \right) \right] \right. \\
&\quad \left. + \left(k_1 - \frac{1}{2} \right) \left(\frac{|x_2|}{\pi_1} \right) \left[v_r \cos \left(\frac{x_1}{m\pi_1} \right) - v_{\min} \right] \right\} \\
&\leq \pi_2 \left(k_1 - \frac{1}{2} \right) v_r \frac{1}{m} \left| \frac{\cos \left(\frac{x_1}{m\pi_1} \right) - \cos \left(\frac{\bar{x}_0}{m} - \frac{x_1}{m\pi_1} \right)}{\frac{|\bar{x}_0|}{m}} \right| \\
&\leq \sqrt{2} \left(k_1 - \frac{1}{2} \right) (v_{\max} - \epsilon_v) \frac{1}{M_0} M_2
\end{aligned}$$

where the last inequality comes from $1/m < 1/M_0$, $\pi_2 < \sqrt{2}$ since $0 < |\bar{x}_0| < 1$, and (21) by letting $\alpha = \bar{x}_0/m$ and $\beta = x_1/m\pi_1$.

2) $x_2 < 0$. Noting that $v_{\max} - v_r \cos(\bar{x}_0/m - x_1/m\pi_1) \geq \epsilon_v$ and $(v_{\min} + \epsilon_v) \cos(x_1/m\pi_1) - v_{\min} \leq \epsilon_v$ we get that

$$\begin{aligned}
& \frac{\pi_2}{|\bar{x}_0|} (\sigma_1 u_1 + \sigma_2) \\
&= \frac{\pi_2}{|\bar{x}_0|} \left\{ \left(k_1 - \frac{\bar{x}_0 x_1}{\pi_2 \pi_1^2} \right) \left(-\frac{|x_2|}{\pi_1} \right) \right. \\
&\quad \times \left[v_{\max} - v_r \cos \left(\frac{\bar{x}_0}{m} - \frac{x_1}{m\pi_1} \right) \right] + \gamma_2 \left(k_1 - \frac{1}{2} \right) \\
&\quad \times \left. \left(\frac{x_2}{\pi_1} \right)^2 \left[(v_{\min} + \epsilon_v) \cos \left(\frac{x_1}{m\pi_1} \right) - v_{\min} \right] \right\} \\
&\leq \frac{\pi_2}{|\bar{x}_0|} \left\{ \left(k_1 - \frac{1}{2} \right) \left(-\frac{|x_2|}{\pi_1} \right) \epsilon_v + \gamma_2 \left(k_1 - \frac{1}{2} \right) \left(\frac{|x_2|}{\pi_1} \right) \epsilon_v \right\} \\
&\leq 0.
\end{aligned}$$

The second term in (27) can be bounded as follows:

$$\begin{aligned}
\frac{\pi_2}{|\bar{x}_0|} \sigma_3 &\leq \frac{\pi_2}{|\bar{x}_0|} \left[k_1 v_r \left(\frac{x_1}{\pi_1} \right) \sin \left(\frac{\bar{x}_0}{m} - \frac{x_1}{m\pi_1} \right) \right. \\
&\quad \left. + k_1 v_r \left(\frac{x_1}{\pi_1} \right) \sin \left(\frac{x_1}{m\pi_1} \right) \right] \\
&\leq \pi_2 k_1 v_r \left| \frac{x_1}{\pi_1} \right| \frac{1}{m} \left| \frac{\sin \left(\frac{\bar{x}_0}{m} - \frac{x_1}{m\pi_1} \right) + \sin \left(\frac{x_1}{m\pi_1} \right)}{\frac{|\bar{x}_0|}{m}} \right| \\
&\leq \sqrt{2} k_1 (v_{\max} - \epsilon_v) \frac{1}{M_0} M_1
\end{aligned}$$

where the first inequality comes from $(x_1/\pi_1) \sin(x_1/m\pi_1) \geq 0$ according to (15),

and the last inequality comes from $\pi_2 < \sqrt{2}$, $1/m < 1/M_0$, and (20) by letting $\alpha = \bar{x}_0/m$ and $\beta = x_1/m\pi_1$.

The third term in (27) can be bounded as follows:

$$\begin{aligned}
\frac{\pi_2}{|\bar{x}_0|} \sigma_4 &= \frac{\pi_2}{|\bar{x}_0|} \frac{\bar{x}_0}{\pi_2} \left[\frac{x_2}{\pi_2} \omega_r + \frac{1+x_2^2}{\pi_1^3} v_r \sin \left(\frac{\bar{x}_0}{m} - \frac{x_1}{m\pi_1} \right) + \gamma_0 \frac{\bar{x}_0}{\pi_2} \right] \\
&\leq \left| \frac{x_2}{\pi_1} \omega_r \right| + \left| \frac{1+x_2^2}{\pi_1^3} v_r \sin \left(\frac{\bar{x}_0}{m} - \frac{x_1}{m\pi_1} \right) \right| + \gamma_0 \left| \frac{\bar{x}_0}{\pi_2} \right| \\
&\leq (\omega_{\max} - \epsilon_\omega) + (v_{\max} - \epsilon_v) + \gamma_0.
\end{aligned}$$

Combining these expressions gives the desired result.

Case 3) $\bar{x}_0 = 0$. In this case we have $\dot{V} + W_3 = \sigma_1(u_1 + \sigma_2) + \sigma_3$. For σ_3 we have

$$\begin{aligned}
\sigma_3 &= k_1 \left(\frac{x_1}{\pi_1} \right) \sin \left(\frac{x_1}{m\pi_1} \right) [\gamma_1 (v_{\min} + \epsilon_v) - v_r] \\
&\leq k_1 \left(\frac{x_1}{\pi_1} \right) \sin \left(\frac{x_1}{m\pi_1} \right) v_r (\gamma_1 - 1) \leq 0.
\end{aligned}$$

From (28)

$$u_1 = \begin{cases} v_{\min} - v_r \cos \left(\frac{x_1}{m\pi_1} \right) & x_2 \geq 0 \\ v_{\max} - v_r \cos \left(\frac{x_1}{m\pi_1} \right) & x_2 < 0. \end{cases} \quad (32)$$

Consider the following two cases with regard to x_2 .

1) $x_2 \geq 0$. Similar to Case 2, we get that

$$\begin{aligned}
\sigma_1 u_1 + \sigma_2 &= k_1 \left(\frac{|x_2|}{\pi_1} \right) \left[v_{\min} - v_r \cos \left(\frac{x_1}{m\pi_1} \right) \right] + \gamma_2 \left(k_1 - \frac{1}{2} \right) \\
&\quad \times \left(\frac{x_2}{\pi_1} \right)^2 \left[(v_{\min} + \epsilon_v) \cos \left(\frac{x_1}{m\pi_1} \right) - v_{\min} \right] \\
&\leq k_1 \left(\frac{|x_2|}{\pi_1} \right) \left[v_{\min} - v_r \cos \left(\frac{x_1}{m\pi_1} \right) \right] \\
&\quad + \gamma_2 k_1 \left(\frac{|x_2|}{\pi_1} \right) \left[v_r \cos \left(\frac{x_1}{m\pi_1} \right) - v_{\min} \right] \\
&= (\gamma_2 - 1) k_1 \left(\frac{|x_2|}{\pi_1} \right) \left[v_r \cos \left(\frac{x_1}{m\pi_1} \right) - v_{\min} \right]
\end{aligned}$$

which is nonpositive since $0 < \gamma_2 < 1$ and $m > 1/\cos^{-1}(v_{\min}/(v_{\min} + \epsilon_v))$.

2) $x_2 < 0$. Similar to Case 2, we get that

$$\begin{aligned}
\sigma_1 u_1 + \sigma_2 &= k_1 \left(-\frac{|x_2|}{\pi_1} \right) \left[v_{\max} - v_r \cos \left(\frac{x_1}{m\pi_1} \right) \right] + \gamma_2 \left(k_1 - \frac{1}{2} \right) \\
&\quad \times \left(\frac{x_2}{\pi_1} \right)^2 \left[(v_{\min} + \epsilon_v) \cos \left(\frac{x_1}{m\pi_1} \right) - v_{\min} \right] \\
&\leq k_1 \left(-\frac{|x_2|}{\pi_1} \right) \epsilon_v + \gamma_2 k_1 \left(\frac{|x_2|}{\pi_1} \right) \epsilon_v \\
&\leq (\gamma_2 - 1) k_1 \left(\frac{|x_2|}{\pi_1} \right) \epsilon_v
\end{aligned}$$

which is also nonpositive. \blacksquare

APPENDIX II

PROOF OF LEMMA 6

Define

$$M_3 \triangleq \max \left\{ 0, \sup_{\substack{0 < |\alpha| < 1 \\ |\beta| < 1 \\ 0 < \vartheta < 1}} (\alpha^2 + 1) \frac{\rho_1}{\alpha^2} \right\} \quad (33)$$

$$M_4 \triangleq \max \left\{ 0, \sup_{\substack{0 < \alpha < 1 \\ |\beta| < 1}} (\alpha^2 + 1) \frac{\rho_2}{\alpha^2} \right\} \quad (34)$$

$$M_5 \triangleq \max \left\{ 0, \sup_{0 < |\alpha| < 1} (\alpha^2 + 1) \frac{\rho_3}{\alpha^2} \right\} \quad (35)$$

where

$$\rho_1 = \left(k_1 \beta + \frac{\alpha}{\sqrt{\alpha^2 + 1}} \vartheta \right) \sin \left(\frac{\alpha - \beta}{m} \right) + k_1 \gamma_1 \beta \sin \left(\frac{\beta}{m} \right)$$

$$\rho_2 = \frac{|\alpha|}{\sqrt{\alpha^2 + 1}} (\omega_{\max} - \epsilon_\omega) + \left(k_1 - \frac{1}{2} \right) \left[v_{\min} - (v_{\min} + \epsilon_v) \cos \left(\frac{\alpha - \beta}{m} \right) \right] + \gamma_2 \left(k_1 - \frac{1}{2} \right) \left[(v_{\min} + \epsilon_v) \cos \left(\frac{\beta}{m} \right) - v_{\min} \right]$$

$$\rho_3 = \frac{|\alpha|}{\sqrt{\alpha^2 + 1}} (\omega_{\max} - \epsilon_\omega) + \left(k_1 - \frac{1}{2} \right) (\gamma_2 - 1) \epsilon_v$$

and k_1, γ_1, γ_2 , and m are defined in Theorem 4.

It is easy to see that M_3, M_4 , and M_5 in (33), (34), and (35) are bounded as $|\alpha|$ approaches 1. Note that $1 < (\alpha^2 + 1) < 2$ since $0 < |\alpha| < 1$. For (33), two cases will be considered with regard to β . In the case of $\beta = 0$, $(\alpha^2 + 1)\rho_1/\alpha^2 = (\sqrt{\alpha^2 + 1})\vartheta \sin(\alpha/m)/\alpha$, which is bounded by $1/m$ as α approaches 0. In the case of $\beta \neq 0$, as $|\alpha|$ approaches 0, ρ_1 approaches $k_1(\gamma_1 - 1)\beta \sin(\beta/m)$, which is negative since $0 < \gamma_1 < 1$ and $|\beta/m| < 1/m < \pi/4$ following (15). Thus, $M_3 = 1/m$ as $|\alpha|$ approaches 0. For (34), as $|\alpha|$ approaches 0, ρ_2 approaches $(k_1 - 1/2)(\gamma_2 - 1)[(v_{\min} + \epsilon_v) \cos(\beta/m) - v_{\min}]$, which is also negative following (16). Thus, $M_4 = 0$ as $|\alpha|$ approaches 0. For (35), as $|\alpha|$ approaches 0, ρ_3 approaches $(k_1 - 1/2)(\gamma_2 - 1)\epsilon_v$, which is also negative. Thus, $M_5 = 0$ as $|\alpha|$ approaches 0. Therefore, M_3, M_4 , and M_5 are finite and can be found by straightforward numerical techniques.

Define

$$\kappa_\omega = \max \left\{ 2\omega_{\max} - \epsilon_\omega, \frac{d_3}{m-1}, \frac{d_4}{m-1} \right\} \quad (36)$$

$$\kappa_v = \frac{\omega_{\max} - \epsilon_\omega}{2k_1 - 1} + \gamma_2 \epsilon_v \quad (37)$$

where

$$d_3 = M_3(v_{\max} - \epsilon_v) + \gamma_0 + \frac{1}{2}(\omega_{\max} - \epsilon_\omega)$$

$$d_4 = M_3(v_{\max} - \epsilon_v) + \gamma_0 + \max\{M_4, M_5\}.$$

Proof to lemma 6: Obviously $k_{\text{sat}}(t, x)$ satisfies the first and third conditions in Theorem 5. We will show that it also stays in the feasible control set $\mathcal{F}(t, x)$, that is, $\dot{V} = (\partial V / \partial x)(f_1 + g_1 k_{\text{sat}}(t, x)) \leq -W(x)$.

Note that

$$\dot{V} + W(x) = \delta_1 + \delta_2 + \delta_3 + \delta_4 \quad (38)$$

where

$$\delta_1 = k_1 \left(\frac{x_1}{\pi_1} \right) \left[v_r \sin \left(\frac{\bar{x}_0}{m} - \frac{x_1}{m\pi_1} \right) + \gamma_1 (v_{\min} + \epsilon_v) \sin \left(\frac{x_1}{m\pi_1} \right) \right] + \frac{\bar{x}_0}{\pi_2} \frac{1 + x_2^2}{\pi_1^3} v_r \sin \left(\frac{\bar{x}_0}{m} - \frac{x_1}{m\pi_1} \right)$$

$$\delta_2 = \frac{\bar{x}_0}{\pi_2} \left(m - \frac{x_2}{\pi_1} \right) u_0 + \gamma_0 \left(\frac{\bar{x}_0}{\pi_2} \right)^2$$

$$\delta_3 = \frac{\bar{x}_0}{\pi_2} \frac{x_2}{\pi_1} \omega_r$$

$$\delta_4 = \left(k_1 - \frac{\bar{x}_0 x_1}{\pi_2 \pi_1^2} \right) \left(\frac{x_2}{\pi_1} \right) u_1 + \gamma_2 \left(k_1 - \frac{1}{2} \right) \left(\frac{x_2}{\pi_1} \right)^2 \times \left[(v_{\min} + \epsilon_v) \cos \left(\frac{x_1}{m\pi_1} \right) - v_{\min} \right].$$

Four cases will be considered as follows.

Case 1) $-\eta_\omega \bar{x}_0 \notin [\underline{v}, \bar{v}]$ **and** $-\eta_v x_2 \notin [\underline{v}, \bar{v}]$. In this case, the saturation functions are the same as the discontinuous signum like functions in Theorem 4, which implies that $\dot{V} \leq -W(x)$ in this case.

Case 2) $-\eta_\omega \bar{x}_0 \in [\underline{v}, \bar{v}]$ **and** $-\eta_v x_2 \in [\underline{v}, \bar{v}]$. In this case, we can see that $u_0 = -\eta_\omega \bar{x}_0$ and $u_1 = -\eta_v x_2$. We also know that $|\bar{x}_0| < 1$ since $\eta_\omega > \kappa_\omega \geq 2\omega_{\max} - \epsilon_\omega$.

Noting that

$$\delta_1 \leq M_3 (v_{\max} - \epsilon_v) \left(\frac{\bar{x}_0}{\pi_2} \right)^2 \quad (39)$$

$$\delta_2 \leq [-(m-1)\eta_\omega + \gamma_0] \left(\frac{\bar{x}_0}{\pi_2} \right)^2 \quad (40)$$

$$\delta_3 \leq \frac{1}{2} \left[\left(\frac{\bar{x}_0}{\pi_2} \right)^2 + \left(\frac{x_2}{\pi_1} \right)^2 \right] (\omega_{\max} - \epsilon_\omega) \quad (41)$$

$$\delta_4 \leq \left(k_1 - \frac{1}{2} \right) (\gamma_2 \epsilon_v - \eta_v) \left(\frac{x_2}{\pi_1} \right)^2 \quad (42)$$

where (39) comes from (33) by letting $\alpha = \bar{x}_0$, $\beta = x_1/\pi_1$, and $\vartheta = (1 + x_2^2)/\pi_1^3$, and (41) follows Young's Inequality. Therefore,

$$\dot{V} + W(x) \leq [d_3 - (m-1)\eta_\omega] \left(\frac{\bar{x}_0}{\pi_2} \right)^2 + \left[\frac{1}{2}(\omega_{\max} - \epsilon_\omega) + \left(k_1 - \frac{1}{2} \right) (\gamma_2 \epsilon_v - \eta_v) \right] \left(\frac{x_2}{\pi_1} \right)^2$$

which is nonpositive since $\eta_\omega > \kappa_\omega \geq d_3/(m-1)$ and $\eta_v > \kappa_v = (\omega_{\max} - \epsilon_\omega)/(2k_1 - 1) + \gamma_2 \epsilon_v$.

Case 3) $-\eta_\omega \bar{x}_0 \in [\underline{v}, \bar{v}]$ **and** $-\eta_v x_2 \notin [\underline{v}, \bar{v}]$. In this case, $|\bar{x}_0| < 1$, δ_1 and δ_2 follow the same inequalities (39) and (40), and $\delta_3 \leq (|x_2|/\pi_1)(|\bar{x}_0|/\pi_2)(\omega_{\max} - \epsilon_\omega)$. Note that $\underline{v} < 0$ from the property of m and $\bar{v} \leq \epsilon_v$. If $-\eta_v x_2 < \underline{v}$, we can get that $x_2 > -(\underline{v}/\eta_v) > 0$. Thus, $(\delta_3 + \delta_4) \leq (|x_2|/\pi_1)M_4(\bar{x}_0/\pi_2)^2 \leq M_4(\bar{x}_0/\pi_2)^2$. If $-\eta_v x_2 > \bar{v}$, we can get that $x_2 < -(\bar{v}/\eta_v) < 0$. Thus, $(\delta_3 + \delta_4) \leq$

$|x_2/\pi_1| M_5(\bar{x}_0/\pi_2)^2 \leq M_5(\bar{x}_0/\pi_2)^2$. Therefore, $\dot{V} + W(x) \leq 0$ since $\eta_\omega > \kappa_\omega \geq d_4/(m-1)$.

Case 4) $-\eta_\omega \bar{x}_0 \notin [\underline{\omega}, \bar{\omega}]$ and $-\eta_v x_2 \in [\underline{v}, \bar{v}]$. In this case, $u_0 \text{sign}(\bar{x}_0) \leq -\epsilon_\omega$ and δ_4 follows the same inequality (42). It can be seen that $(\sigma_1 u_1 + \sigma_2) \triangleq \delta_4 \leq 0$ since $\eta_v > \kappa_v > \gamma_2 \epsilon_v$. We can see that $\dot{V} + W(x) \leq -\epsilon_\omega (|\bar{x}_0|/\pi_2)(m - (x_2/\pi_1) + \sigma_3 + \sigma_4)$. Then following the proof for Theorem 4, we know that $\dot{V} + W(x) \leq 0$ is guaranteed based on the choice of m .

Combining these four cases gives the desired result. ■

REFERENCES

- [1] E. D. Sontag, "A Lyapunov-like characterization of asymptotic controllability," *SIAM J. Control Optim.*, vol. 21, no. 3, pp. 462–471, May 1983.
- [2] Z. Artstein, "Stabilization with relaxed controls," *Nonlinear Anal., Theory, Methods, Applicat.*, vol. 7, no. 11, pp. 1163–1173, 1983.
- [3] D. Q. Mayne and H. Michalska, "Receding horizon control of nonlinear systems," *IEEE Trans. Automat. Contr.*, vol. 35, pp. 814–824, July 1990.
- [4] E. F. Camacho and C. Bordons, *Model Predictive Control*. New York: Springer-Verlag, 1999.
- [5] Y. Lin and E. Sontag, "Control-Lyapunov universal formulas for restricted inputs," *Control Theory Adv. Technol.*, vol. 10, no. 4, pp. 1981–2004, Dec. 1995.
- [6] Y. Lin and E. D. Sontag, "Universal formula for stabilization with bounded controls," *Syst. Control Lett.*, vol. 16, pp. 393–397, June 1991.
- [7] Z.-P. Jiang and H. Nijmeijer, "Tracking control of mobile robots: a case study in backstepping," *Automatica*, vol. 33, pp. 1393–1399, 1997.
- [8] J.-M. Yang and J.-H. Kim, "Sliding mode motion control of nonholonomic mobile robots," *IEEE Control Syst. Mag.*, vol. 19, pp. 15–23, Apr. 1999.
- [9] Z.-P. Jiang, E. Lefeber, and H. Nijmeijer, "Saturated stabilization and track control of a nonholonomic mobile robot," *Syst. Control Lett.*, vol. 42, pp. 327–332, 2001.
- [10] T.-C. Lee, K.-T. Song, C.-H. Lee, and C.-C. Teng, "Tracking control of unicycle-modeled mobile robots using a saturation feedback controller," *IEEE Trans. Contr. Syst. Technol.*, vol. 9, pp. 305–318, Mar. 2001.
- [11] J. W. Curtis and R. W. Beard, "Satisficing: a new approach to constructive nonlinear control," *IEEE Trans. Automat. Contr.*, vol. 49, pp. 1090–1102, July.
- [12] E. P. Anderson and R. W. Beard, "An algorithmic implementation of constrained extremal control for UAVs. presented at the AIAA Guidance, Navigation, and Control Conf. Paper AIAA-2002-4470
- [13] D. Kingston, R. Beard, T. McLain, M. Larsen, and W. Ren, "Autonomous vehicle technologies for small fixed wing UAVs. presented at the AIAA 2nd Unmanned Unlimited Systems, Technologies, and Operations-Aerospace, Land, and Sea Conference and Workshop & Exhibit Paper AIAA-2003-6559
- [14] A. W. Proud, M. Pachter, and J. J. D'Azzo, "Close formation flight control. presented at the AIAA Guidance, Navigation, and Control Conf. Paper AIAA-99-4207
- [15] R. W. Beard, T. W. McLain, M. Goodrich, and E. P. Anderson, "Coordinated target assignment and intercept for unmanned air vehicles," *IEEE Trans. Robot. Automat.*, vol. 18, pp. 911–922, Dec. 2002.
- [16] Y. J. Kanayama, Y. Kimura, F. Miyazaki, and T. Noguchi, "A stable tracking control method for an autonomous mobile robot," in *Proc. IEEE Int. Conf. Robotics and Automation*, Cincinnati, OH, 1990, pp. 384–389.
- [17] E. Sontag and Y. Wang, "New characterizations of input-to-state stability," *IEEE Trans. Automat. Contr.*, vol. 41, pp. 1283–1294, Sept. 1996.
- [18] M. Krstić and H. Deng, *Stabilization of Nonlinear Uncertain Systems*, ser. Communication and Control Engineering. New York: Springer-Verlag, 1998.
- [19] H. K. Khalil, *Nonlinear Systems*, 2nd ed. Englewood Cliffs, NJ: Prentice-Hall, 1996.
- [20] J. R. Cloutier, C. N. D'Souza, and C. P. Mracek, "Nonlinear regulation and nonlinear H_∞ control via the state-dependent Riccati equation technique," in *Proc. IFAC World Congr.*, San Francisco, CA, 1996, pp. 365–370.



robotics.

Wei Ren (SM'97–SM'98) was born in Shaanxi, China, in 1976. He received the B.S. degree in electrical engineering from Hohai University, Nanjing, China, in 1997, and the M.S. degree in electrical engineering from Tongji University, Shanghai, China, in 2000. He is currently working toward the Ph.D. degree in the Department of Electrical and Computer Engineering, Brigham Young University, Provo, UT.

His research interests include cooperative control of multiple vehicle systems, nonlinear control, and



Randal W. Beard (S'91–M'92–S'92–M'95–SM'02) received the B.S. degree in electrical engineering from the University of Utah, Salt Lake City, in 1991, and the M.S. degree in electrical engineering in 1993, the M.S. degree in mathematics in 1994, and the Ph.D. degree in electrical engineering in 1995, all from Rensselaer Polytechnic Institute, Troy, NY.

Since 1996, he has been with the Electrical and Computer Engineering Department, Brigham Young University, Provo, UT, where he is currently an Associate Professor. In 1997 and 1998, he was a Summer Faculty Fellow at the Jet Propulsion Laboratory, California Institute of Technology, Pasadena. His research interests include unmanned air vehicles, coordinated control of multiple vehicle systems, and nonlinear and optimal control.

He is a member of American Institute of Aeronautics and Astronautics and Tau Beta Pi, and is currently an Associate Editor for the *IEEE Control Systems Magazine* and an Associate Editor on the *IEEE Control Systems Society Conference Editorial Board*.